DEVELOPMENT OF A TABLETOP GUIDANCE SYSTEM FOR EDUCATIONAL ROBOTS

C. W. Bac, T. E. Grift, G. Menezes

ABSTRACT. *The guidance of a vehicle in an outdoor setting is typically implemented using a Real Time Kinematic Global Positioning System (RTK-GPS) potentially enhanced by auxiliary sensors such as electronic compasses, rotation encoders, gyroscopes, and vision systems. Since GPS does not function in an indoor setting where educational competitions are often held, an alternative guidance system was developed.*

This article describes a guidance method that contains a laser-based localization system, which uses a robot-borne single laser transmitter spinning in a horizontal plane at an angular velocity up to 81 radians per second. Sensor arrays positioned in the corners of a flat rectangular table with dimensions of 1.22 m × 1.83 m detected the laser beam passages. The relative time differences among the detections of the laser passages gave an indication of the angles of the sensors with respect to the laser beam transmitter on the robot. These angles were translated into Cartesian coordinates. The guidance of the robot was implemented using a uni-directional wireless serial connection and position feedback from the localization system.

Three experiments were conducted to test the system: 1) the accuracy of the static localization system was determined while the robot stood still. In this test the average error among valid measurements was smaller than 0.3 %. However, a maximum of 3.7 % of the measurements were invalid due to several causes. 2) The accuracy of the guidance system was assessed while the robot followed a straight line. The average deviation from this straight line was 3.6 mm while the robot followed a path with a length of approximately 0.9 m. 3) The overall performance of the guidance system was studied while the robot followed a complex path consisting of 33 sub-paths.

The conclusion was that the system worked reasonably accurate, unless the robot came in close proximity (<0.2 m) to one of the sensor arrays where errors occurred due to a high angle of incidence of the laser beam onto the sensor arrays and due to a high tangential velocity of the laser beam at the opposite sensor array. Hence, this article presents a low-cost guidance system which is simple, reliable, and reasonably accurate.

Keywords. *Laser localization, Indoor localization, Laser-based guidance, Robot competition.*

The Global Positioning System (GPS) has become a popular localization method for autonomous vehicles and robots in outdoor environments. With low-cost receivers it is possible to obtain accuracies of up to 3 m, and with differential correction using a private base station the accuracy can be increased to a centimeter level. This method is the basis for the popular 'auto steer' option on agricultural vehicles.

GPS does not function in an indoor setting and therefore participants in robotics competitions, which are often held indoors, lack an affordable guidance method. There are many robotics competitions in existence (Pastor et al., 2008), among which the most prominent FIRST (For Inspiration and Recognition of Science and Technology) Robotics competition (Oppliger, 2001; Chew et al., 2009). However, few exist that have a focus on agriculture. Wageningen University & Research Centre in the Netherlands has organized an Agricultural Robotics competition since 2003 (Van Straten, 2004). The challenges have consisted of variations on the theme of guidance in Maize. The American Society of Agricultural and Biological Engineers (ASABE) hosted its first Robotic Student Design competition in 2007. The main difference between these competitions is that the latter is an indoor event that travels with the Annual International Meeting. This limits the allowable size and weight of the robotic solutions.

In the ASABE robotics competition challenge, usually guidance lines made from black electrical tape are provided, which make the guidance of robots relatively straightforward. Most robots use the LEGO® 'line follower' solution to follow a black electrical tape. A common robot design contains two powered wheels in the front and a caster wheel at the rear. Two optical sensors that can distinguish between the background and the black line are placed beside the black line at the front of the robot. When the right side sensor detects the black line, it turns off the right side motor (or reverses it) which causes the robot to steer to the right, away from the black line. The same procedure is used for the left side. This method causes the robot to move forward while keeping the guidance line between the optical sensors.

Submitted for review in January 2010 as manuscript number IET 8387; approved for publication by the Information & Electrical Technologies Division of ASABE in April 2011.

The authors are **Cornelis Wouter Bac,** Graduate Student, Farm Technology Group, Wageningen University and Research Centre, Wageningen, The Netherlands; **Tony E. Grift, ASABE Member Engineer,** Associate Professor, and **Glen Menezes,** Graduate Research Assistant, Department of Agricultural and Biological Engineering, University of Illinois at Urbana-Champaign, Urbana, Illinois. **Corresponding author:** Tony E. Grift, Department of Agricultural and Biological Engineering, University of Illinois at Urbana-Champaign, 1304 W. Pennsylvania Ave., Urbana, IL 61801; phone: 217-333-2854; e-mail: grift@illinois.edu.

  ISSN 0883-8542

Although several successful competitions have been held, the need to provide guidance lines significantly limits the level of the challenges that can be posed to student teams. If a reliable, low-cost indoor guidance system were available, the challenges can be closer to realistic outdoor applications. The principle of the localization system as proposed in this paper is unique compared to alternatives in its simplicity and cost.

Some commercially available systems targeted at full-scale robots employ optical range finders and the time-of-flight principle (Sohn and Kim, 2008), as well as ultrasound (Wehden et al., 2006). Other methods are based on measuring the signal strength of transmitters, but these are targeted at large distances and have limited accuracy (Elnahrawy et al., 2004). Furthermore, some methods are vision based where a camera is mounted above the robot and image processing is used to determine the actual position of the robot (Hada et al., 2003). An indoor localization system called the NorthStar® (Evolution Robotics™, Pasadena, Calif.) was inspired by a celestial navigation system that has been used for centuries. Here, artificial landmarks are created on a ceiling or wall, and the robots determine their position by processing an image of the landmarks. A similar system is called the Hagisonic Stargazer Robot Localization System (Robotshop, 2009). The latter two methods work accurately and allow for multiple robot localization, but are expensive and complex. As an alternative, Salomon et al. (2006) developed a triangulation method which is related to the method proposed in this article. This system contained sensors mounted in four corners of a table which measured the angle of the sensor with respect to a continuous light beacon mounted on the robot. Gordon (1987) applied a method, similar to the method in this research, in an outdoor setting. At a distance of 120 to 300 m between the transmitter and receiver an accuracy of ±1.2 m was obtained, but the arrangement suffered from measurement errors due to changes in ambient light conditions. The method proposed in this article does not require special sensors, cameras, or image processing algorithms. All system components are commercially available and the (*x, y*) coordinates are obtained through a simple mathematical equation. Most importantly, the system does not require calibration since it was founded on simple sensors, straightforward processing, and a solid mathematical model.

The objectives of this article were: 1) to develop an indoor guidance system targeted at robotics competitions, 2) to test the feasibility, precision, and accuracy of this system.

Materials and Methods

The components of the robot guidance system were a wirelessly controlled robot, as well as an indoor localization system which gave a real-time robot position on a table top. These components will be discussed in detail in the following sections.

Localization System using Three Sensor Arrays

The localization system has three pulse inputs, caused by the laser beam triggering three sensor arrays in the corners of a flat, horizontal table. After processing the pulses by an electronic circuit, the pulse durations (in μs) were converted into a position on the table. An overview of the table with its sensor arrays in corners O, A, and C is given in figure 1.

There are three angles α, β, γ that are measured in the localization system, but in reality only two are required because the third is complimentary to 360°. Therefore, in the derivation only the angles α, β are needed. To obtain the position of the robot *P*(*x, y*), it was necessary to derive a function which converts the measured angles α, β, the constant length of the table *L* in m, and the constant width of the table *W* in m to Cartesian (*x, y*) coordinates as:

$$P(x,y) = f(\alpha,\beta,L,W) \quad (1)$$

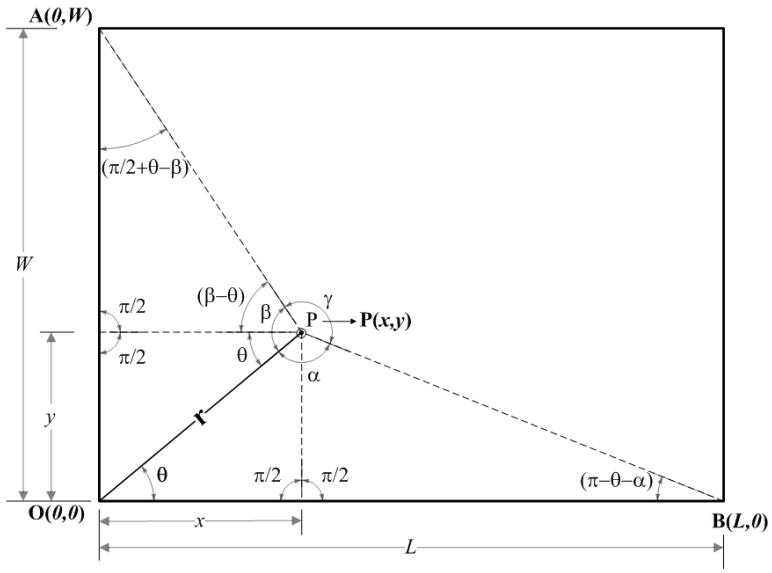

Figure 1. Graphical representation of the table with three sensor arrays placed in the corners. The length of the rectangular table is 1.83 m, and the width is 1.22 m. The laser transmitter was rotating in a counter-clockwise direction around point P and triggered sensor arrays placed in the corners O, A, and B. The pulses produced when the laser transmitter triggered the sensor arrays were used to calculate the (*x, y*) position of point P (Appendix A).

Appendix A gives the complete derivation arriving at the following equations (fig. 1):

$$\left.\begin{aligned}\theta &= \tan^{-1}\left[\frac{L-\frac{W}{\tan\beta}}{-\frac{L}{W\tan\alpha}}\right]\\ r &= \frac{W\cos(\theta-\beta)}{\sin\beta}\end{aligned}\right\} \Rightarrow \begin{cases} x = r\cos\theta \\ y = r\sin\theta \end{cases} \quad (2)$$

Localization System Using Four Sensor Arrays

Although the localization system works by measuring two out of three angles as shown in figure 1, it was decided to add a fourth sensor array for three reasons. Firstly, the redundant sensor allows occlusion of one of the sensor arrays while still producing a valid position measurement. Secondly, the sensor arrays do not always produce a pulse trigger while being struck by the laser beam. This can happen when the tangential velocity of the laser beam passing the sensor array is too high. Thirdly, an angle of incidence between the transmitter and the sensor array decreases the chance of a pulse trigger. The effect of the angle of incidence on a pulse was not investigated.

In conclusion, four sensor arrays improve the reliability of the localization paper. This research was therefore executed with a localization system that was based on four sensor arrays, as shown in figure 2.

Robot

The robot used in the project was a Parallax BOE-bot (Board Of Education®) robot, available in a kit. This differential drive robot (measuring 105 mm × 95 mm) has two drive wheels in the front and a perforated plastic ball that serves as a caster in the rear. The BOE-bot was fitted with a Basic Stamp II microcontroller and can be programmed in a Basic language. To enable wireless control of the robot, a transmitter (443 MHz RF, Parallax, Rocklin, Calif.) was connected to a PC serial port using a MAX232 line driver chip, and a receiver (part no. 27981, Parallax, Rocklin, Calif.) was fitted on the robot. This system only enables downstream communication from a computer to the robot. The robot and parts all originated from Parallax, Rocklin, California (www.parallax.com). Figure 3 shows a photo of the robot, in which the inset on the right shows one of four sensor arrays used in the localization system. The rotating laser transmitter was mounted, by two plastic tie wraps, on the pulley of a Mitsumi 2558A DC motor (Jameco Electronics, Belmont, Calif.). One AA battery was mounted under the robot platform to power the DC motor.

Localization System Hardware

The localization system hardware consisted of a rotating laser transmitter, four sensor arrays, a personal computer, and an electronic circuit. Figure 4 shows an overview of all hardware components that were used in this research.

The class IIIa (<5 mW) laser transmitter has a wavelength of 650 nm and spins in a horizontal plane. An angular velocity had to be selected which resulted in a pulse trigger. In a separate experiment, it was determined that a pulse trigger was produced up to a tangential velocity of 270 m/s, when the laser beam pointed directly at the sensor array, at zero angle of incidence. This angular velocity was found too high because on the table, the laser beam struck the sensor array at a high angle of incidence. Therefore, to guarantee a pulse, even at a high angle of incidence, the angular velocity was limited to 81 rad/s. To achieve this angular velocity, the DC motor was powered at 1.5 V.

Each sensor array consisted of 20 vertically oriented phototransistors (Ligitek LPT2023, Jameco Electronics, Belmont, Calif.) to allow for a vertical deviation of the laser beam. The phototransistors with a diameter of 3 mm were

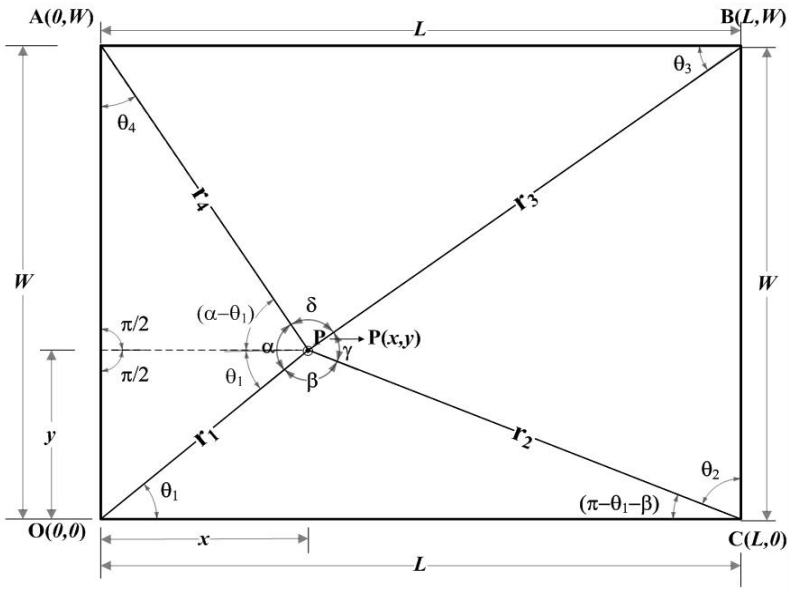

Figure 2. Graphical representation of the table as shown in figure 1, with four sensor arrays in the corners. The redundant fourth array was added to allow for occlusion of one of the sensor arrays and to compensate for errors.

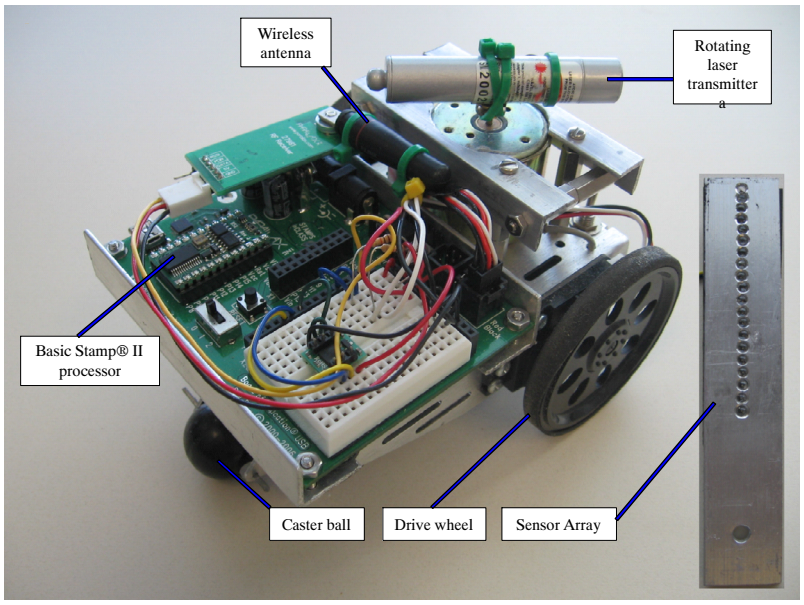

Figure 3. BOE-bot educational robot with the laser transmitter mounted on top.

spaced 4 mm apart (see inset in fig. 3). The phototransistors, commonly used in infrared remote control applications, have peak sensitivity at a wavelength of 940 nm. However, they were found sufficiently sensitive to detect the 650-nm laser light. To obtain sensor arrays that are independent of which phototransistor in the array is triggered by the laser beam, all 20 phototransistors in the array were placed in parallel. The pulses generated by the sensor arrays were processed using an electronic circuit as shown in figure 5.

The four sensor array outputs (collectors of the phototransistors shown on the left) were pulled up to 5 V DC using a circuit containing a 1-kΩ resistor in series with a 2-kΩ trim potentiometer. The 1-kΩ resistor is a safety measure: The 2 kΩ potentiometer can be trimmed to 0 kΩ, and without the safety series resistor the current would not be limited which causes the phototransistor to fail. The 2-kΩ potentiometer provided a means to trim away voltage drops caused by ambient light. The emitters of the phototransistors were all directly connected to ground. The pull-up resistors invert the output, meaning that the output of the sensor array is in a high (5 V) state in idle while producing an analog pulse with an amplitude lower than 1 V when any of the 20 phototransistors in the array was triggered by the laser beam.

To process the analog pulses originating from the phototransistor arrays, they were converted into digital pulses. This was achieved by feeding the pulses into a LM399 (National Semiconductor) comparator chip. The reference voltage for the comparator chip was provided at half the supply voltage, using a voltage divider containing two identical 3.3-kΩ resistors.

The output of the circuit as shown in figure 5, consists of four consecutive pulses T_1, T_2, T_3, and T_4. Their durations were translated into the angles α, β, γ, and δ as shown in figure 2 using the mathematical equations as derived in Appendix A. This was achieved by channeling the digital output pulses from the LM399 comparator chip into four 'set'

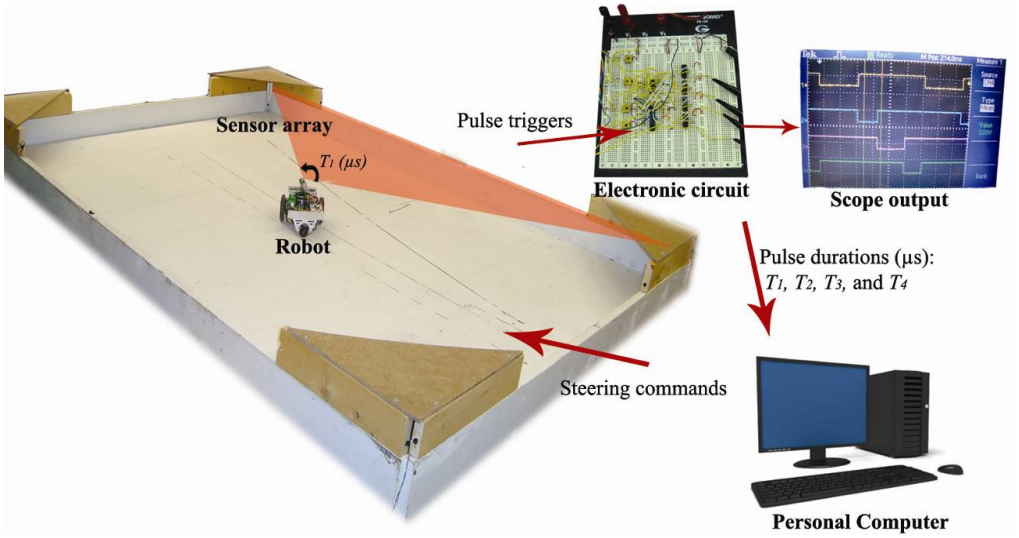

Figure 4. Overview of the hardware components used in this research. The PC calculated the position and orientation of the robot and used it to send steering commands to the microprocessor on the robot. The sensor arrays were shielded against disturbances from varying ambient light conditions.

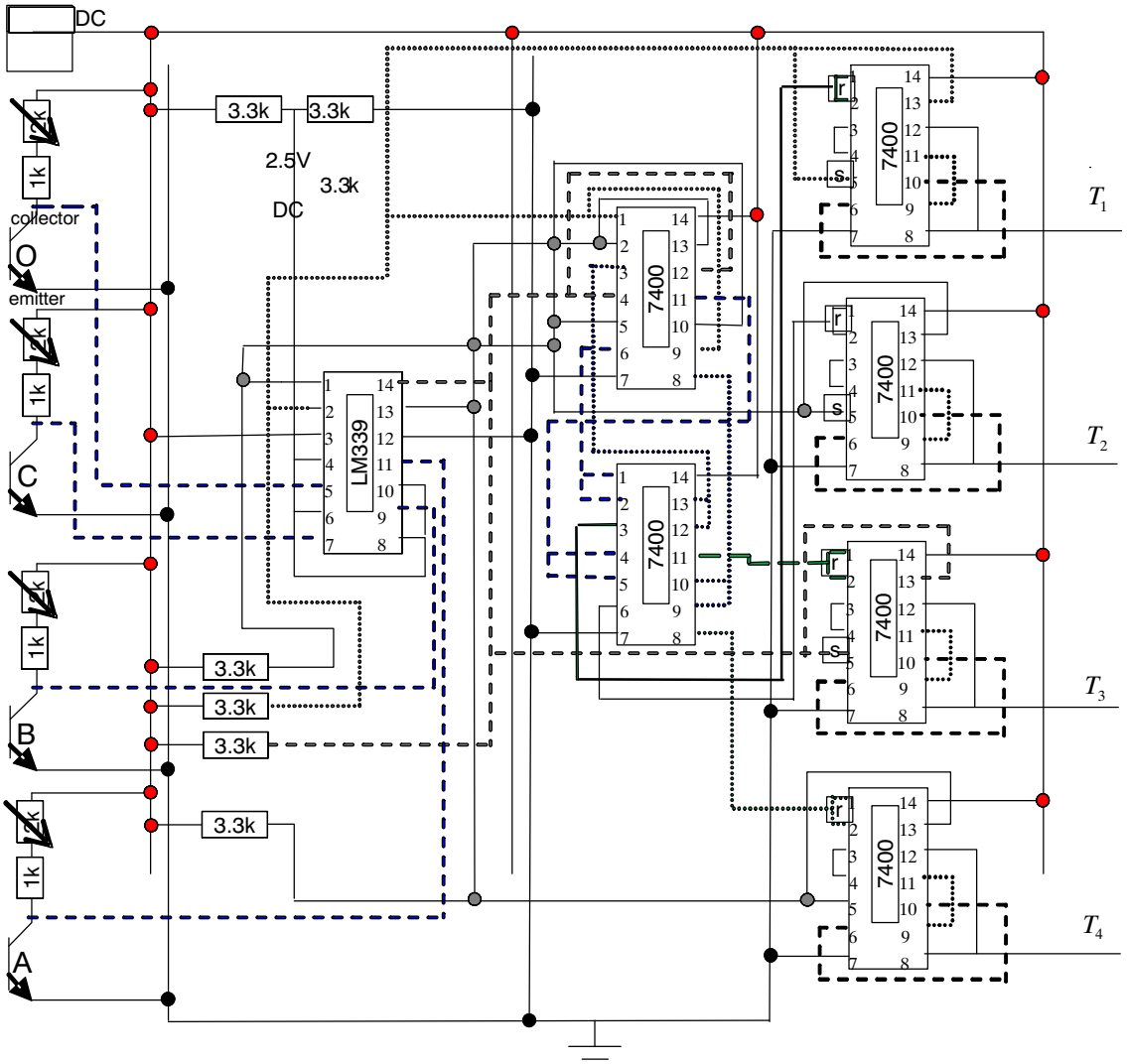

Figure 5. Electronic circuit of the signal processing unit. The phototransistors on the left each represent an array of 20 phototransistors connected in parallel. The 2-kΩ trim potentiometers allow compensating for ambient light falling on the sensors. The LM 339 acts as a comparator which converts analog pulses from the phototransistors into digital pulses. The 'r' and 's' symbols at the 7400 NAND gates indicate 'reset' and 'set'.

and 'reset' latches realized in TTL 7400 NAND gates. Figure 6 shows an oscilloscope image of the consecutive active low pulse outputs T_1, T_2, T_3, and T_4 of the four latches shown in figure 5.

If all four sensor arrays are triggered by the laser beam, the negative flank of each consecutive pulse resets the previous latch to a high logical state. In other words, T_2 resets T_1, T_3 resets T_2, T_4 resets T_3, and T_1 resets T_4 . The width of a 'low' pulses represents the time in ms between the triggering of two consecutive sensor arrays. The sum of the four 'low' pulse widths constitutes the time needed for one complete 360° laser rotation in ms. The durations of the four consecutive pulses T_1, T_2, T_3, and T_4 were measured using a PCI-6601 counter / timer board (National Instruments, Austin, Tex.) with a clock frequency of 20 MHz under control of a program written in LabVIEW® 8.6.

Because the system has four instead of the three required sensor arrays, it can yield a valid position value even if one of the sensor arrays is occluded, implying that one of the four time pulses (T_1, T_2, T_3, or T_4) is missing. In this case, the system uses the remaining three pulses to determine the position of the robot. If for instance pulse T_2 in figure 6 would

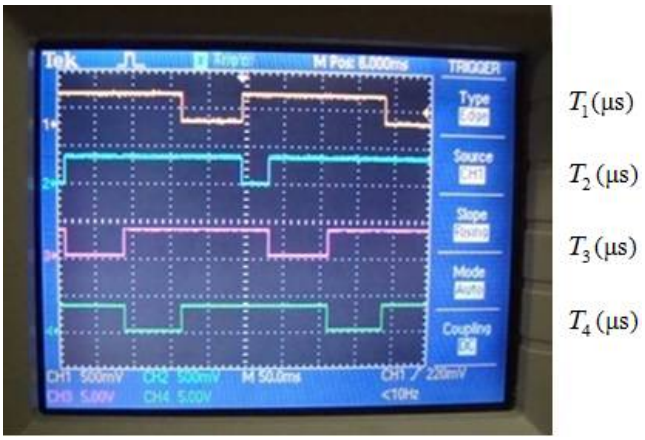

Figure 6. Oscilloscope image showing four consecutive pulses representing the pulse durations (µs) T_1, T_2, T_3, and T_4. The pulses can be translated into the corresponding angles α, β, γ, and δ in figure 2.

be missing, the duration of pulse T_1 would be short and the position erroneous. To correct for the missing pulse T_2, T_1 and T_2 are summed. Hence, T_1 is now extended to the start of

pulse T_3. This was accomplished by a 'reset' pulse that is fired when pulse T_3 is 'set' (negative flank). This means that T_1 can be reset to a logical high state by a 'set' signal from either T_2 or T_3, in other words, if T_2 does not reset T_1, T_3 will. This mechanism was carried forward to deal with any of the four timing pulses being absent: The electronic circuit (fig. 5) used two TTL 7400 NAND gates to realize this functionality.

The electronic circuit as shown in figure 5 ensures that in the case of a single missing pulse, the position can be determined based on the three remaining valid pulses, but the position can only be determined if it is known which of the pulses was missing. To determine this, a time-out value was defined in the 'timer Express-VI' in LabVIEW® 8.6. When no pulse update was received by the timer within the time-out limit, which was set to 130 ms, LabVIEW® 8.6 assigned 0 s to the missing measurement. Subsequently, an if-then-else statement determined which pulse was missing and executed one of four corresponding localization code segments.

Localization Algorithm

The processing of the pulses and the determination of the position $P(x, y)$ was performed in a LabVIEW® program, which consists of four steps:

- measure the duration of the pulses as shown in figure 5 using four timers in the PCI 6601 board,
- determine which, if any, of the pulses are missing after a complete rotation of the laser transmitter,
- calculate the position using the formula that relates the measured pulse durations (translated into angles) to the Cartesian position $P(x, y)$, and
- determine the orientation of the robot using consecutive positions.

Because the robot did not have an orientation sensor, the orientation was determined by evaluating two consecutive positions obtained from the localization system. This was carried out only when the distance between two consecutive positions was larger than 1 cm, otherwise inaccurate orientation calculations would occur due to measurement errors in the (x, y) position.

Guidance

Guidance of the robot was performed by a uni-directional wireless communication link through which commands were sent to the robot. Because the only actuators on the robot were the two drive wheels, only the forward/backward velocity and rate of turn were controlled. In LabVIEW® a combination of three numbers was created to send commands to the robot. The number combination indicated whether the robot should rotate left or right and through how many degrees. The angle of rotation was calculated by comparing the orientation needed to reach the goal coordinate following a straight line, with the current robot orientation. The guidance procedure can be described by the following steps:

- The current robot position is compared to the current goal coordinate. When the robot is located within a radius of 3 cm from the goal coordinate, a new goal coordinate was taken from a pre-defined array.
- A correction was sent if the goal orientation deviated more than 0.05 radians from the actual robot orientation.
- When the robot moves in the desired direction, it will drive straight. No commands were sent until the deviation from the goal orientation became larger than 0.05 rad or when a new goal coordinate was taken from the pre-defined array.

Filtering Erroneous Measurements

During the motion of the robot, erroneous measurements occurred. The first type of erroneous measurement occurred in the hardware. One error was that occasionally the measured duration of any pulse was added to the next pulse duration. If, for example, pulse T_1 and T_2 read 15 and 20 ms, respectively, T_2 was occasionally processed as 35 ms, resulting in an unrealistic (x, y) position. The cause of this hardware error is unknown and occurred in about 3.4% of all incoming measurements. Secondly, the laser angular velocity was not constant while the robot turned. During a turn, the laser angular velocity either decreases or increases. The mathematical derivation assumes a constant laser angular velocity and a velocity change therefore resulted in an erroneous (x, y) position.

A straightforward approach was used to filter both types of errors. The total time of a laser rotation was compared to a manually defined value. When the manually defined value differed too much from the measured time of a laser rotation, the calculated (x, y) position was deleted. The algorithm selected the smallest pulse duration of the four measured pulse durations T_1, T_2, T_3, and T_4 as a difference tolerance between the manually defined value and the measured total time of a laser rotation.

Experiments

The robotic guidance system was tested in several ways. Firstly, the accuracy of the static guidance system was evaluated. Secondly, the accuracy evaluation during a straight line motion test was tested. Thirdly, a test was conducted where the robot followed a predefined complex path consisting of 33 sub-paths.

Accuracy of the Static Guidance System

The static accuracy of the localization system was determined while the robot stood still. The measured pulse durations T_1, T_2, T_3, and T_4 as well as the calculated (x, y) positions were stored in a file. These calculated (x, y) positions were compared with the manually measured (x, y) position of the laser transmitter. This manual measurement was conducted using a measuring tape with a resolution of 1 mm.

Accuracy of the Guidance System During Motion

To assess the straight line following performance of the guidance system, 10 coordinates with constant y-values were defined on the table. To determine the true positions of the robot, a whiteboard marker was attached to the robot. The robot positions while following the straight line were measured using the laser localization system and stored, which allowed offline comparisons with the true positions from the whiteboard marker trace.

Guidance of the Robot Along a Predefined Path

The tabletop guidance system was demonstrated at the Annual International Meeting of the American Society of Agricultural & Biological Engineers (ASABE), 21-24 June

2009 in Reno, Nevada. For the demonstration, a composite path was defined that read 'ASABE' (1.2 m × 0.6 m). The complete acronym 'ASABE' consisted of a series of 33 straight-line sub-paths. The guidance approach, which could be applied to any predefined path, employed proportional control on the robot orientation.

A path-planning algorithm was implemented with the purpose of following the 33 predefined straight sub-paths that define the complete ASABE acronym. The robot switched to the next predefined goal coordinate when it reached a position within 5 cm of the desired coordinate.

To follow the pre-defined paths, two steering modes were employed depending on the deviations between the actual and the desired orientation values. Equation 3 shows the first steering mode u_{rot}, where turning was performed by holding one wheel and turning the other.

$$u_{rot} = \frac{\theta - \theta_{goal}}{\pi} u_{rot\_\pi} \quad (3)$$

where

θ = actual orientation value (rad),

θ_{goal} = desired orientation value (rad),

u_{rot_π} = turning rate to execute an anti-clockwise rotation of π rad.

The turning rate u_{rot} determines the angle through which the robot should turn to reach the desired orientation θ_{goal}. This first steering mode was used for deviations from θ_{goal} that were smaller than 0.3 rad and larger than 0.05 rad. The value of 0.05 rad was chosen to create a dead band for robot control which has the advantage of eliminating overshoot and a faster response to control inputs.

The first steering mode u_{rot} allowed the robot to follow the path more quickly, at small deviations from θ_{goal}, compared to the second steering mode u_{turn}. Equation 4 shows this second mode u_{turn}, where the wheels turned in opposite direction at equal velocity to allow enable a spin-turn.

$$u_{turn} = \frac{\theta - \theta_{goal}}{\pi} u_{turn\_\pi} \quad (4)$$

where

u_{turn_π} = turning rate to execute an anti-clockwise turn of π rad.

The second steering mode was used for deviations from θ_{goal} that were larger than 0.3 rad. A spin-turn was more effective for such large deviations because the robot turned around the center of the robot. As a result, fewer steering corrections were needed to reach the goal orientation θ_{goal}.

Extreme turns would occur for measured orientations of approximately 6.2 rad and a goal orientation of 0. Heuristics were implemented to compensate for this problem.

The method of employing the two steering modes increased the overall driving velocity of the robot. However, this approach has the disadvantage of not compensating for external disturbances: In practice the robot will slip during a rotation and several rotation commands are needed to achieve the desired orientation.

Results and Discussion

Based on 864 measurements, the average values and the standard deviation of the static laser position are presented in table 1. The true position of the spinning laser transmitter was measured as 1.16 ± 0.01 m for the *x*-position and as 0.53 ± 0.01 m for the *y*-position.

From table 1 it is clear that the stationary localization system is precise because the standard deviation of the correct measurements is lower than 0.3% from the average. It is also clear that the differences in the average position of three-sensor measurements compared to four-sensor measurements are negligible, in other words both three- and four-sensor measurements are adequate to calculate the position.

Among five static experiments, the number of filtered errors varied between 1% and 3.7% of the total measurements. The number of measured values for each experiment was in the range of 700 to 1,000 measurements. Besides these errors, erroneous measurements occurred because the voltage drop at the receiver was too small to create a pulse: If this occurs at two receivers during a single rotation of the laser transmitter, position determination is impossible. This type of error only occurred when the robot is in close proximity (<0.2 m) to one of the sensor arrays. This causes a high angle of incidence on all sensor arrays, and in addition causes a high laser beam tangential velocity at the sensor array at the opposite side of the table. In the center of the table, all four receiver arrays yielded a measurable pulse.

In the experiment where the robot followed a predefined straight path parallel to the *x*-axis, the robot was started with both wheels set to move at the same velocity. However, this is no guarantee that the robot will follow a perfectly straight line and therefore, a whiteboard marker was attached to observe the true path of the robot. The coordinates from the localization system were recorded during the run, and the deviations from the observed path recorded. Figure 7 shows the recorded positions superimposed onto the path observed with the whiteboard marker.

It is clear from figure 7 that the robot follows the straight line reasonably well because the deviations from the straight path had a standard deviation of 3.6 mm across the travel distance of approximately 0.9 m.

A final experiment consisted of the robot following a composite path which spelled out the acronym 'ASABE'. The robot was started at position (0.56, 0.35) and the average velocity of the robot was 0.1 m/s with a peak velocity of 0.14 m/s. The laser angular velocity was 81 rad/s. The results of this experiment are shown in figure 8.

Table 1. Performance evaluation of the stationary localization system.

	No.	Average *x*-position (mm)	Average *y*-position (mm)	Standard Deviation *x*-position (mm)	Standard Deviation *y*-position (mm)
Erroneous measurements	6	839.6	303.6	665.1	242.3
Correct measurements	1444	1159.0	529.5	1.7	1.7
Four-sensor measurements	637	1160.0	528.6	0.7	1.6
Three-sensor measurements	807	1158.2	530.3	0.2	0.1

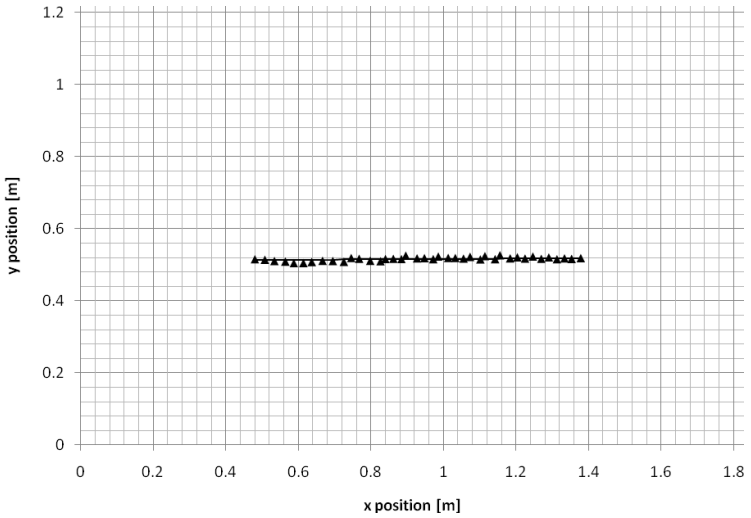

Figure 7. Forty measured (*x*, *y*) coordinates for a straight path followed by the robot. The angular velocity of the laser was 31 rad/s. The peak velocity of the robot was 0.17 m/s and the average velocity was 0.12 m/s. The standard deviation of the deviations from the straight path in the y-direction was 3.6 mm.

From figure 8 it is evident that the robot followed the 'ASABE' path reasonably well, although in some areas errors occurred. In the center of the board, the system worked accurately, but in the areas where the robot is in close proximity (<0.2 m) to one of the sensor arrays (in the corners of the table) the accuracy can become rather low. For instance, in the top right corner of figure 8, errors can be seen, because the robot is close to the top right sensor array.

The outlier above the letter "E," was caused by a hardware error for which the authors do not have an explanation, other than potential optical laser reflections. Unfortunately, this outlier was not filtered. This outlier caused the robot to turn to an undesired orientation. The correct orientation was recalculated after the next two (*x*, *y*) positions.

The processing speed of the Basic Stamp® II microprocessor (Parallax, Rocklin, Calif.) was another limiting factor in smooth control of the robot. The personal computer is able to send commands to the robot every 200 ms, but in practice the Basic Stamp® II microprocessor was not able to process this volume of commands. Besides the limiting processing speed, the communication rate of the serial wireless communication was limited to 4,800 baud. Therefore, a dead band was implemented to avoid missing too many control commands. The limitations imposed by the processing speed could be reduced by lowering the driving velocity of the robot; however, this would come at the cost of a reduced orientation update frequency.

The angular velocity of the laser transmitter was 81 rad/s. During motion, a higher angular velocity would increase the accuracy of the localization, but this would also increase the tangential velocity of the laser beams on the receiver arrays, increasing the chance of missing pulses altogether. Therefore, the safest way to increase the accuracy of the system is to limit the driving velocity of the robot.

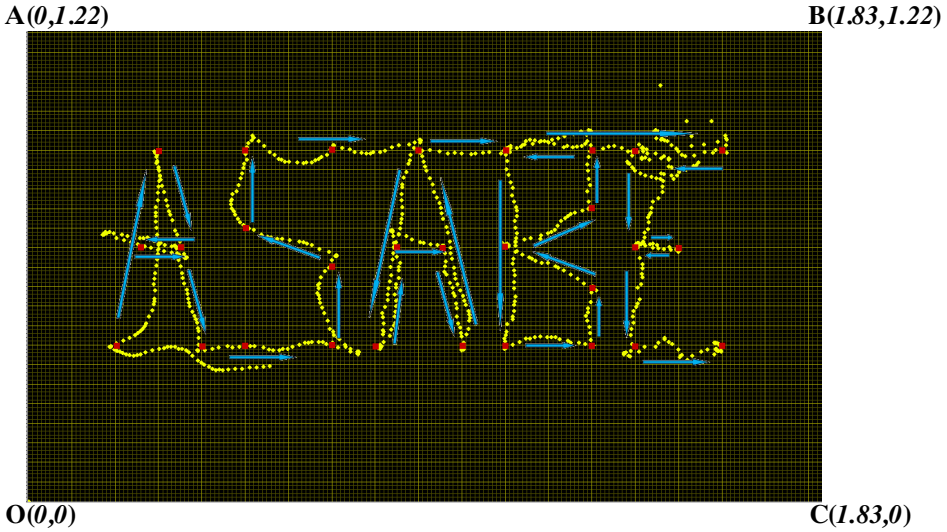

Figure 8. Path based on an array of 33 coordinates representing the letters 'ASABE'. The target coordinates are shown as dots. The initial position was set to (0.56; 0.35). The robot drove in the direction of the arrows while maintaining an average velocity of 0.10 m/s, with a peak velocity of 0.14 m/s. The laser angular velocity was 81 rad/s.

Conclusions

A laser-based robot guidance system was developed which consisted of a BOE-Bot educational robot, a laser transmitter spinning in a horizontal plane with an angular velocity of up to 81 rad/s and four sensor arrays placed in the corners of a table. The timing among the sensor arrays being triggered by the laser beam allowed for calculation of the instantaneous robot position. The robot was guided by sending steering commands through a wireless data link. Two modes of steering were employed.

The overall feasibility of the guidance system was evaluated in three experiments: The first evaluated the performance of a stationary localization subsystem. The second evaluated the straight line performance of the system and the third demonstrated the robot performance while following a complex series of 33 sub-paths which in combination made up the letters 'ASABE'. The following conclusions were drawn from these experiments.

- Static experiments showed that the localization system is accurate with a standard deviation among correct measurements within 0.3% from the average position. Erroneous measurements occurred at a maximum rate of 3.7% of all incoming measurements. These erroneous measurements were detected and discarded. Additional erroneous measurements occurred when the robot was in close proximity (<0.2 m) to one of the sensor arrays placed in the corners of the table.
- In a dynamic experiment where the robot followed a predefined straight path resulted in an average deviation from the path of 3.6 mm, among 40 measurements recorded while traveling through a distance of 0.9 m.
- The final experiment consisted of the robot following 33 consecutive sub-paths which in combination made up the words 'ASABE'. This experiment confirmed that the accuracy of the complete system was good as long as the robot was located in the center of the table, at a distance of at least 0.2 m from the sensor arrays. Furthermore, similar to the static experiments, erroneous position observations occurred when the robot was in close proximity (<0.2 m) to one of the sensor arrays.
- The limited processing and communication speed of the system posed problems in the guidance of the robot. To alleviate the problem a dead band was imposed, which relaxed the behavior of the robot, but also made it less responsive.

Recommendations and Further Research

To improve the performance of the complete guidance system some parts need to be redesigned and improved. For instance, the current optical subsystem consists of a 650-nm laser transmitter in combination with phototransistor with a peak sensitivity at 940 nm. A matched combination would improve the optical subsystem of the localization system.

To reduce the error sensitivity at the edges of the table, rotating sensor arrays could be designed. Such a change would reduce errors that occur due to an angle of incidence on the sensor array. However, it would require an additional controller on each sensor array.

Adding sensors to the robot would improve the guidance system. For instance, adding an electronic compass would give a more direct orientation measurement. Adding sensors to the robot would however require a bi-directional data link, whereas in the current design a uni-directional link sufficed.

To control the robot better, instead of relying solely on the instantaneous data from the localization system, a Kalman filter could be applied. This would improve the overall performance and robustness of the guidance system.

References

Chew, M. T., S. Demidenko, C. Messom, and G. S. Gupta. 2009. Robotics competitions in engineering education. In *Proc. 4th Intl. Conf. on Autonomous Robots and Agents*, 624-627. Wellington, New Zealand.

Elnahrawy, E., X. Li, and R. P. Martin. 2004. The limits of localization using signal strength: A comparative study. In *Proc. 2004 1st Annual IEEE Communications Society Conf. on Sensor and Ad Hoc Communications and Networks*, 406-414. New York: IEEE.

Gordon, G. P. 1987. Laser position locating system for off-road vehicles. M.Sc. thesis. Ohio State University. Available at: http://etd.ohiolink.edu/send-pdf.cgi/Gordon%20Greg%20P.pdf?osu1200512216. Accessed Aug. 14, 2011.

Hada, Y., E. Hemeldan, K. Takase, and H. Gakuhari. 2003. Trajectory tracking control of a nonholonomic mobile robot using iGPS and odometry. In *Proc. of IEEE Intl. Conf. on Multisensor Fusion and Integration for Intelligent Systems,* 51-57. New York: IEEE.

Langdon, M. 2009. Child's play: Learning robotics. *Eng. and Tech.* 4(3): 42-45.

Oppliger, D. E. 2001. University - Pre College interaction through FIRST robotics competition. In *Proc. Intl. Conf. on Engineering Education (ICEE'2001)*, 11-15, Oslo/Bergen, Norway. Available at: http://www.ineer.org/events/icee2001/proceedings/papers/273.pdf. Accessed Aug. 14, 2011.

Pastor, J., I. Gonzalez, and F. J. Rodríguez. 2008. Participating in an international robot contest as a way to develop professional skills in engineering students. In *38th ASEE/IEEE Frontiers in Education Conf.,* 9-14. New York: IEEE.

Robotshop. 2009. Hagisonic StarGazer Robot Localization System. Available at: www.robotshop.us/hagisonic-stargazer-localization-system-2.html. Accessed 13 January 2010.

Salomon, R., M. Schneider, and D. Wehden. 2006. Low-cost optical indoor localization system for mobile objects without image processing. In *Proc. IEEE Conf. on Emerging Technologies and Factory Automation*, 629-632. New York: IEEE.

Sohn, H. J., and B. K. Kim. 2008. An efficient localization algorithm based on vector matching for mobile robots using laser range finders. *J. Intelligent and Robotic Systems: Theory and Applications* 51(4): 461-488.

Van Straten G. 2004. Field robot event, Wageningen, 5-6 June 2003. *Computers and Electronics in Agric.* 42: 51-58.

Wehden, D., R. Salomon, and M. Schneider. 2006. Low cost sonic-based indoor localization for mobile robots. In *Proc. 3rd Workshop on Positioning, Navigation, and Communication (WPNC'06)*, 53-58, Hannover, Germany. Shaker Verlag.

APPENDIX A

Conversion of Angles Relative to Sensor Array Positions in the Corners of the Table to Cartesian Coordinates.

From figure 3, applying the sine rule to Δ(APO) yields:

$$\frac{r}{\sin\left(\frac{\pi}{2}+\theta-\beta\right)}=\frac{W}{\sin(\beta)} \tag{5}$$

Applying the sine rule for Δ(BPO) yields:

$$\frac{r}{\sin(\pi+\theta-\alpha)}=\frac{L}{\sin\alpha} \tag{6}$$

Combining (5) and (6) gives:

$$r=W\frac{\sin\left(\frac{\pi}{2}+\theta-\beta\right)}{\sin\beta}=L\frac{\sin(\pi-\theta-\alpha)}{\sin\alpha} \tag{7}$$

Because $\sin(\pi-\theta-\alpha)=\sin(\theta+\alpha)$, and $\sin\left(\frac{\pi}{2}+\theta-\beta\right)=\cos(\theta-\beta)$ it follows:

$$W\left[\frac{\cos(\theta-\beta)}{\sin\beta}\right]=L\left[\frac{\sin(\theta+\alpha)}{\sin\alpha}\right] \tag{8}$$

Applying sum and difference formulas for sine and cosine gives:

$$\frac{W}{\sin\beta}\left[\cos\theta\cos\beta+\sin\theta\sin\beta\right]=\frac{L}{\sin\alpha}\left[\sin\theta\cos\alpha+\cos\theta\sin\alpha\right] \tag{9}$$

Dividing by sinβ in the left term and sinα in the right term, given that $\frac{\sin\varphi}{\cos\varphi}=\tan\varphi$ yields:

$$\left[\frac{W\cos\theta}{\tan\beta}+W\sin\theta\right]=\left[\frac{L\sin\theta}{\tan\alpha}+L\cos\theta\right] \tag{10}$$

Collecting sinθ on the left and cosθ on the right gives:

$$\sin\theta\left[W-\frac{L}{\tan\alpha}\right]=\cos\theta\left[L-\frac{W}{\tan\beta}\right] \tag{11}$$

Solving for θ gives:

$$\frac{\sin\theta}{\cos\theta}=\tan\theta=\left[\frac{L-\frac{W}{\tan\beta}}{W-\frac{L}{\tan\alpha}}\right] \tag{12}$$

Leading to:

$$\theta=\tan^{-1}\left[\frac{L-\frac{W}{\tan\beta}}{W-\frac{L}{\tan\alpha}}\right] \tag{13}$$

Because θ is now known, based on the constant length *L* and width *W* combined with the measured α, β, the radius *r* can be computed from equation 5 with the equality $\sin\left(\frac{\pi}{2}+\theta-\beta\right)=\cos(\theta-\beta)$.

$$r=W\frac{\cos(\theta-\beta)}{\sin\beta} \tag{14}$$

Because the distance *r* and angle θ are known from equation 13 and equation 14, from figure 1 it follows that:

$$\begin{aligned} x&=r\cos\theta\\ y&=r\sin\theta \end{aligned} \tag{15}$$